NanoSIMS study of organic matter associated with soil aggregates: advantages, limitations and combination with STXM.

*LAURENT REMUSAT **

Laboratoire de Minéralogie et Cosmochimie du Muséum, UMR 7202 CNRS/MNHN, Muséum National d'Histoire Naturelle, case postale 52, 57 rue Cuvier, 75231 Paris Cedex 05, France. remusat@mnhn.fr

PIERRE-JOSEPH HATTON

INRA, Laboratoire de Biogéochimie des Ecosystèmes Forestiers, UR 1138, INRA Nancy, 54280 Champenoux, France. Pierre-Joseph.Hatton@nancy.inra.fr

PETER S. NICO

Earth Sciences Division, Lawrence Berkeley National Laboratory, Berkeley, CA, 94720, USA. psnico@lbl.gov

BERND ZELLER

INRA, Laboratoire de Biogéochimie des Ecosystèmes Forestiers, UR 1138, INRA Nancy, 54280 Champenoux, France. zeller@nancy.inra.fr

MARKUS KLEBER

Department of Crop and Soil Science, Oregon State University, Corvallis, OR-97331, USA.

markus.kleber@oregonstate.edu

DELPHINE DERRIEN

INRA, Laboratoire de Biogéochimie des Ecosystèmes Forestiers, UR 1138, INRA Nancy, 54280 Champenoux, France. delphine.derrien@nancy.inra.fr

*: corresponding author. Tel: +33 1 40 79 81 42; Fax +33 1 40 79 57 72. Email: remusat@mnhn.fr

Abstract: Direct observations of processes occurring at the mineral-organic interface are increasingly seen relevant for the cycling of both natural soil organic matter and organic contaminants in soils and sediments. Advanced analytical tools with the capability to visualize and characterize organic matter at the sub-micron scale, such as Nano Secondary Ion Mass Spectrometry (NanoSIMS) and Scanning Transmission X-ray Microscopy (STXM) coupled to Near Edge X-ray Absorption Fine Structure Spectroscopy (NEXAFS) may be combined to locate and characterize mineral-associated organic matter. Taking advantage of samples collected from a decadal ^{15}N litter labeling experiment in a temperate forest, we demonstrate the potential of NanoSIMS to image intact soil particles and to detect spots of isotopic enrichment even at low levels of ^{15}N application. We show how microsites of isotopic enrichment detected by NanoSIMS can be speciated by STXM-NEXAFS performed on the same particle. Finally, by showing how ^{15}N enrichment at one microsite could be linked to the presence of microbial metabolites, we emphasize the potential of this combined imaging and spectroscopic approach to link microenvironment with geochemical process and/or location with ecological function.

TOC Art

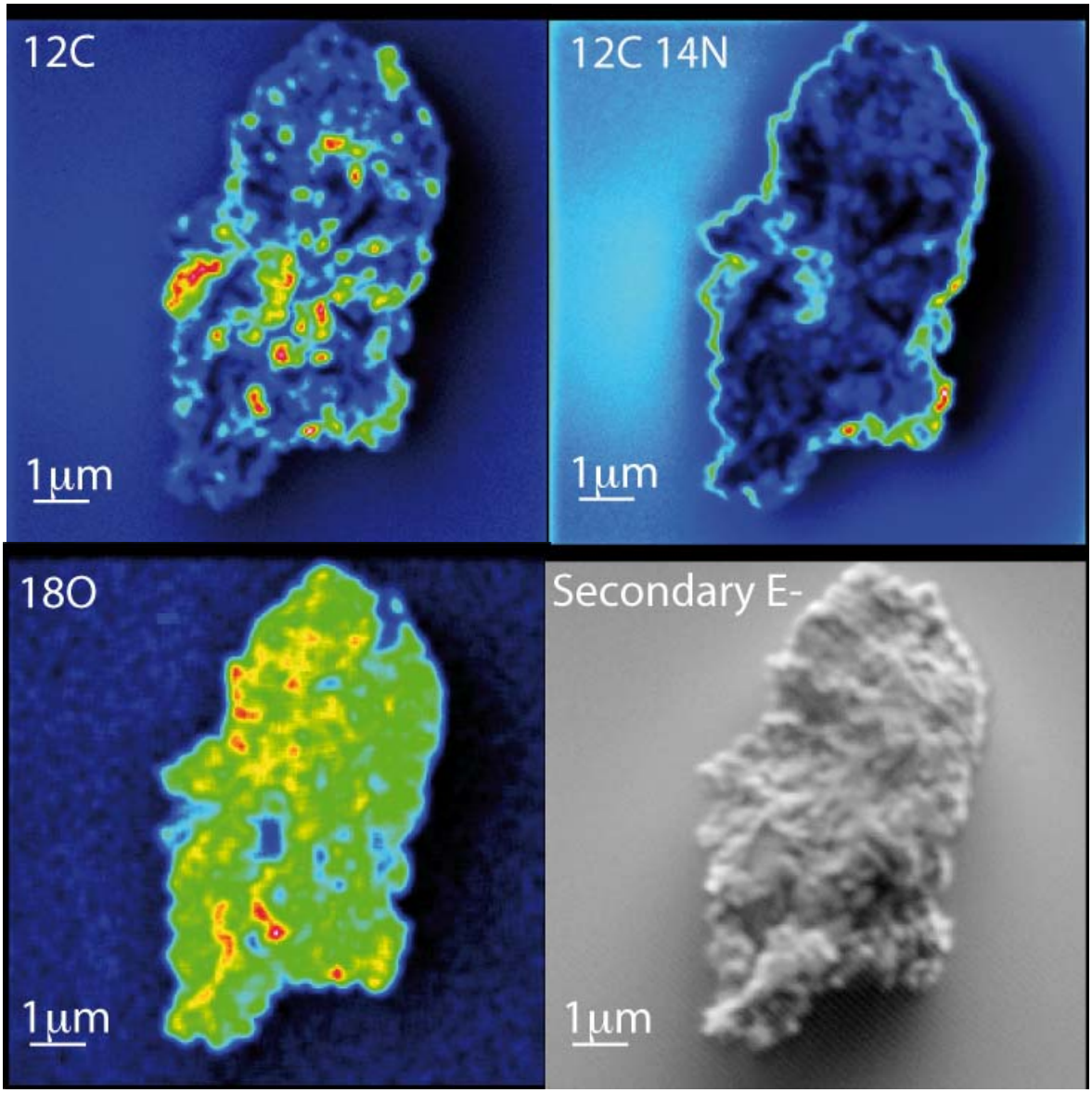

Introduction:

The spatial distribution of organic matter (OM) within the soil matrix has major consequences for its accessibility to decomposers [1]. When mineral particles entrap or come in close association with OM, they build physical barriers that prevent decomposer organisms and exo-enzymes from accessing OM and decrease the *in situ* supply of gas, water and nutrients. A useful simplification divides the processes of mineral-organic interaction into two major categories. Organic matter can a) become occluded by aggregated soil structures, and/or b) be engaged in fine scale interactions with mineral surfaces through the activity of microorganisms [2] and a variety of adsorption mechanisms [3, 4]. To date, investigations into the fate of such mineral associated organic materials are restricted to procedures of bulk analysis performed on operationally defined physical fractions. They are expected to isolate mineral-organic associations of given characteristics, such as an increasing proportion of microbially processed organic matter in fractions of increasing density [5-7]. Nevertheless, all physical fractionation techniques in use today involve some level of interference with the spatial integrity of soil microenvironments while there is an increasing awareness of a strong dependence of geochemical process intensity on the physical structure of the mineral matrix.

The development of micron to nano-scale techniques now opens the gate to elemental, isotopic and molecular characterization at the required scale to shed new lights on organo/mineral associations. Nano Secondary Ion Mass Spectrometry (NanoSIMS) provides elemental and isotopic maps of OM at the surface of mineral particles with a spatial resolution less than 100 nm [8-10] and permits tracking of isotopically labeled substrates added to the soil [11-14]. In contrast to bulk isotopic measurements by conventional techniques, NanoSIMS allows the visualization of the spread and dilution level of the label into the soil matrix. Previous NanoSIMS studies in soil science have been performed on samples embedded in epoxy and further polished to create surfaces without topography. However, studies on undisturbed microaggregates mounted without carbon-based chemicals are mandatory for applications that are focused on questions of OM turnover and contaminant degradation.

Scanning X-Ray Transmission Microscopy/ Near Edge X-Ray Absorption Fine Structure (STXM/NEXAFS) can determine the speciation of OM at the nano-scale [15-18]. Because STXM and

NanoSIMS operate at similar scales, they should theoretically provide complementary information about organic matter in soil microstructures, provided that samples have (i) intact spatial structure and are (ii) unaffected by embedding organic resins. Initial attempts towards this goal have recently been reported for tiny (micron-size) grains recovered from the coma of comet Wild 2 by the Stardust mission [19]. Our objective with this study is to demonstrate the potential and the limitation of NanoSIMS imaging for (1) tracking OM and labeled residues within soil microaggregates deposited on a clean surface, without any epoxy resin. We further use STXM/NEXAFS to (2) assess the nature of this labeled OM and (3) evaluate the information NanoSIMS can provide on the distribution of a ^{15}N-label within microaggregates. Our conceptual approach was to take advantage of the availability of physical soil separates collected from a forest soil in which ^{15}N-labeled litter had been applied 12 years before sampling.

Experimental Methods

The soil was isolated from forest topsoil located at Ebrach in Germany (49°52' N, 10°27' E). It is classified (World Reference Base) as an acidic dystric Cambisol with a sandy loam texture [20]. ^{15}N labeled leaves were deposited 12 years before sampling (initial A^{15}N of incubated leaves was 2.48%, corresponding to $\delta^{15}N \approx 5785‰$ relative to the atmospheric N_2 standard). Physical fractions were obtained by density fractionation in order to isolate microaggregates. Organic matter within individual fractions was found to vary in the degree of microbial processing and carbon content [21]: microstructures from the 1.8-2.0 g cm^{-3} density fraction are more plant-like (C/N= 16, $\delta^{13}C$=-27‰ relative to PDB) and contain 210 mg C / g of fraction, those found in the 2.2-2.4 g cm^{-3} density fractions show a more microbial-like signature (C/N= 11.5, $\delta^{13}C$=-26‰) with a C content of 38 mg C / g of fraction. ^{15}N tracer applied a decade before sampling was found in both fractions: $\delta^{15}N$ values were 25.2±0.5‰ in the 1.8-2.0 g cm^{-3} density and 25.6±0.2‰ in the 2.2-2.4 g cm^{-3} density fraction, whereas $\delta^{15}N$ of unlabeled aggregates was -3.6±0.1‰ in the lighter fraction and -0.3±0.1‰ in the denser. More details and interpretation for the recovery of ^{15}N label in the microaggregates are available in [21].

An aliquot of each density fraction was deposited onto clean Si_3N_4 windows without the use of any fixative; particles are held in place by plain electrostatic forces. When samples were jointly studied with STXM-NEXAFS and NanoSIMS, they were first imaged by STXM-NEXAFS, because NanoSIMS beam damage is much more severe than that associated with STXM-NEXAFS.

STXM-NEXAFS analyses were performed at beamline 5.3.2 at the Advanced Light Source (ALS), Lawrence Berkeley National Laboratory, Berkeley, USA. Images were obtained by collecting stacks in the X-rays energy region of 278 eV to 330 eV for carbon NEXAFS and in the region of 390 eV to 440 eV for nitrogen NEXAFS. We omitted particles exhibiting an optical density greater than 2.0 at any energy between 278 eV and 290eV, i.e. the main energy range of our carbon K-edge spectra. Those particles were considered to be non-transparent to X-rays, with an effective thickness larger than 150 nm; the thickness limit depends on energy and will be greater at higher energies. Data were processed with the software package aXis2000 to generate STXM images and NEXAFS spectra for selected regions of interest [22].

NanoSIMS imaging was performed at MNHN Paris, France. Prior to NanoSIMS analysis, samples were gold coated (20nm) to improve lateral charge compensation. Imaging was performed using a primary Cs^+ beam with a current set to 0.6 pA (using D1-3) to achieve an actual analytical spatial resolution of less than 100 nm. The primary beam stepped over the sample in a 256 x 256 pixel raster with a speed set at 2 ms/pixel. Secondary ions images of $^{12}C^-$, $^{13}C^-$, $^{18}O^-$, $^{26}CN^-$ and $^{27}CN^-$ were simultaneously collected by electron multipliers. The images cover areas from 64 to 225 μm². The secondary mass spectrometer was tuned for ~6800 mass resolving power (Cameca definition for NanoSIMS) to resolve isobaric interferences (like at mass 27 between $^{12}C^{15}N$ and $^{13}C^{14}N$). Secondary electrons were also simultaneously collected in order to image the sample while we collect secondary ions. Several frames were collected and stacked to increase counting rate and reduce statistical error. Instrumental fractionation was corrected for isotopic ratios using terrestrial type III kerogen, an organic standard with properties similar to the unlabeled SOM ($\delta^{15}N$=3.7±0.2‰). Data were processed as quantitative isotopic ratio images and were corrected for instrumental bias including image drift from

layer to layer (due to drift in the location of the ion beam from frame to frame). $\delta^{13}C$ maps did not reveal any significant enrichment over natural abundance, confirming that the method used in this study did not generate procedural isotope enrichment in our images. Prior to each image acquisition, the sample surface was pre-sputtered using a high current beam (around 70 pA) to remove surface contamination and gold coating and to reach sputtering steady state. As a result, several 100s of nanometers are removed before the analysis. This means that a preexisting thin coating of the particle would be only visible at its edge, the center of the particle representing regions that are several 100s of nm below the surface of the microaggregates.

Detailed procedure for soil fractionation, sample preparation, technical settings for each technique and statistics are described in the supplementary online information.

Results and Discussion

1. NanoSIMS investigation of soil microaggregates deposited on a Si_3N_4 window

Figure 1 shows a microaggregate of approximately 10 by 3 micron size that originated from a physical fraction dominated by plant-like organic materials [21]. In this image, ^{12}C and ^{26}CN are considered to represent OM, whereas ^{18}O signals are assigned to phyllosilicates, primary silicate minerals or pedogenic oxides; ^{18}O yield being higher in mineral than in organic matrices. N is detected as the molecular CN^- ion due to high ionization potential to form N^- under the Cs beam, resulting in a much lower yield in N^- compared to CN^- [23, 24]. As expected the OM appears to be heterogeneously distributed: it occurs as a very thin coating, or as patches in subsurface layers, possibly in protective pores. Nitrogen and Carbon locations differ significantly, indicating a variable OM composition (see figure S1). Carbon is distributed in patches all over the particle, while N is found in some patches and forms a discontinuous rim around the particle.

We need to consider possible sources of analytical bias to discuss the C and N distributions. Microaggregate roughness can be a potential source of bias because sample topography affects the NanoSIMS yield for $^{12}C^-$ and $^{26}CN^-$ ions, preventing us from obtaining accurate C/N ratios [25]. However, on the X-Y profile (Fig. S1) we find no correlation between the amplitude of secondary

electrons (indicative of the topography) and $^{12}C^-$ and $^{26}CN^-$ signals. This allows us to exclude an influence of sample roughness on the distribution of N and C.

There is also the possibility that the $^{26}CN^-$ signal at the edges of the particle may be an artifact produced by the N-rich window. Scattering effects or wrong definition of the region of interest (ROI) may result in a fake rim. The X-Y profile through this particle (see Fig S1) proves that the $^{26}CN^-$ signal at the rim matches with the edge of the particle (indicated by the secondary electron signal) and that the CN^- signal is more intense at the particle rim than on the Si_3N_4 window. Scattering of the primary Cs beam [26, 27] could skew the location of N rich areas in our configuration. When primary Cs ions hit the side of a particle, some may be deviated to the Si_3N_4 window and sputter it, potentially leading to of the appearance of a fake N-rich layer around the particle. This effect is nevertheless small if the particle is constituted by light elements, inducing a small scattering effect because they absorb Cs ions more easily. We believe that we can rule out this effect here because: 1) on the secondary electron image (Figure 1), the microaggregate is rather flat with a roughness smaller than its lateral extension, it should not be thicker than a couple of microns and is composed of light elements (silicates and OM); such particles are not expected to induce significant scattering; 2) The $^{26}CN^-$ rich rim is discontinuous, like on the top side of the particle: the CN^- coating is absent whereas the aspect of the particle is similar to other side regions; there is no reason scattering would not happen in this region in contrast to the rest of the edge of the particle, the primary beam in the NanoSIMS being quasi-perpendicular to the surface. On the other hand, it seems possible that an OM coating could have been cut off in some places during sample preparation. In addition, in another imaging study not involving STXM imaging, we have deposited similar soil microaggregates on cleaned N-free gold foil and the same N-rich rim could also be observed (see an example in Figure S2). Finally, re-deposition of N-rich material around the particle during the Cs sputtering can be excluded here because it would occur outside the imaged area where the Cs beam does not raster.

We conclude that the observation of a N-rich coating, in this case, is not biased and reflects the actual occurrence of OM containing more N-rich moieties than most of the OM of this microaggregate. This

N-rich OM also seems to occur in one area in the middle of grain in a pore (as revealed by a hole in $^{18}O^-$ image) that could have been connected to the outer part of the microaggregate. Clear determination of the origin of this OM is, however, hampered by the lack of information at the molecular scale.

2. NanoSIMS characterization of OM containing a ^{15}N tracer

The amount of ^{15}N tracer was low in our samples collected from a decadal, in-situ labeling experiment: the microaggregates contained about 10mg.g^{-1} N, with ^{15}N representing only 0.3705% of the total N (very close to 0.3655%, the mean natural abundance of ^{15}N). Nevertheless, NanoSIMS successfully detected several cases of ^{15}N-enriched OM among 20 studied particles (Figure 1): the $\delta^{15}N$ map indicates three locations of ^{15}N rich organic materials (See SI and Figure S3 for a description of the statistics used to identify ^{15}N-rich hotspots). In spite of the small size of these regions of interest (around 400 nm wide), the degree of isotopic enrichment is significant even when considerable natural variability is assumed, with $\delta^{15}N$ up to 500‰ whereas natural OM is around $\delta^{15}N$=-2‰. The occurrence of such enriched ^{15}N spots is not compatible with an intense microbial recycling of labeled residues over the 12 year incubation; an intense recycling would have diluted the isotopic signal and spread it over the soil components. As a result, the spots of ^{15}N-rich organic matter are either unaltered residues of the original labeled litter incubated for 12 years or stabilized products of the recycling of this litter. Unfortunately, C/N ratios determined by NanoSIMS in the course of this study are not accurate enough to distinguish between any of the two hypotheses.

A molecular investigation at a similar scale is desirable to assess the fate of the organic label in such a long-term experiment. Characterization at the molecular level is usually achieved by using NMR or GC-MS but these techniques do not provide information about the spatial distribution of molecular moieties at the micron scale.

3. Combined investigation of labeled soil microaggregates by STXM and NanoSIMS

Figure 2 shows images successively acquired on both STXM and NanoSIMS for a five micron-wide microaggregate from the fraction characterized by microbial organic matter [21]. On NanoSIMS images, OM appears only as a thick coating around a side of the particle (Fig. 2B) while STXM

mapping detects OM within a larger zone (Fig. 2C). This illustrates that NanoSIMS and STXM do not image the sample in the same way. NanoSIMS, as a surface technique, can only probe the (sub)surface over a few tens of nm, whereas STXM is a transmission technique that averages information over the entire thickness of the sample. While OM located on the back of the sample will be invisible for NanoSIMS, it contributes to the signal obtained by STXM. For this reason, comparisons between STXM and NanoSIMS images need to account for the fact that the STXM/NEXAFS signal may indicate the presence of more organic species than are present in the thin surface layer probed by NanoSIMS. Only areas with concomitant NanoSIMS and STXM signals (like areas 1 and 2 in figure 2) should be taken into account for joined interpretations. Area 1 is identified by both techniques as being composed of a type of OM that differs from the rest of the organic coating around the aggregate. On NanoSIMS images, this area appears to be very C-rich and could correspond to carbonized OM. The C-NEXAFS spectrum extracted for this area reveals a broad and strong absorption band around 285.2 eV produced by aromatic C and a second distinct peak at 288.5 eV in the carboxylic region. The dominance of the aromatic peak is suggestive of black carbon (BC), and, in fact the major features of this spectrum can be well reproduced by a 58% and 44% linear combination of two reference char spectra, Fescue grass charred at 300°C and 700°C respectively, [28]. In the σ* and post-edge normalization range, >290.5 eV, the shape of the two spectra remain similar although the absolute intensity is different. As this range is very sensitive to normalization and thickness effects, the fact that the lower energy resonances can be well matched by sample BC spectra remains strong evidence for the carbon in the particle being derived from BC. In contrast, the rest of the OM of this particle, as sampled in areas 2 and 3, shows a smaller peak of aromatic material (285.2eV) and noticeable resonances at 288.5eV and 289.3 eV. The region 2 spectrum has the same overall shape of standard spectrum of Tall Fescue grass [28], despite a slight shift to lower energy by 0.14 eV. Even without this shift, the very high degree of similarity implies a potential plant material origin of this spectrum. The region 3 spectrum shows the same features as the region 2 spectrum with additional intensity at 287.2 eV. Solomon, et al [16] assigned the 287.3 region to aliphatic carbon. Similarly, Brandes et al [15] identified the aliphatic

region as 287.1 to 287.4 eV. The increased intensity in this region of the #3 spectrum indicates a greater concentration of aliphatic carbon.

Figure 3 shows the images we successively obtained by both techniques on a particle with a ^{15}N rich hot spot (Fig. 3, region 1). This particle was from a density fraction enriched with microbial products [21]. The ^{15}N-rich hot spot has a $\delta^{15}N$ value of 213±132‰ (2 sigma). According to NanoSIMS and STXM investigations, it is located in a N-poor region (see panel A and C). The feature in the C-NEXAFS spectrum extracted from this area has a relatively broad absorbance band, ranging from 287.8eV to 288.9 ev, centered at 288.3 eV, and peaking at 288.5eV. The 288.7ev to 288.8eV range is taken by Kinyangi et al. [17] to indicate carboxyl-C with amide type features resonating at the lower energy side of this range at 288.2 [29]. The broad nature of this feature in the sample spectrum combined with the lack of large resonances in the aromatic (285.2 eV) region or other prominent features, makes the most likely interpretation of this peak to be a mixture of carbon containing a large fraction of carboxylic/amide functional groups consistent with a mixture of proteins, amino-sugars, and acid containing polysaccharides. The ^{15}N rich hot spot is more consistent with microbial body material and/or exo-polysaccacarides than it is with fresh plant litter material as seen in Figure 2 or in [30] (see the comparison in Fig 3). This is also supported by the comparison with data acquired on pure microbial cells [31]. These results are consistent with the hypothesis that the potential ^{15}N enrichment in this location originates from microbial metabolites produced from the decomposition of the ^{15}N-rich litter rather than a fragment of the litter itself.

It should be cautionary noted that fine scale mixing between several organic pools (like a little amount of labeled plant material embedded in a larger unlabeled blob of microbial material) may remain an issue. A greater number of observations at the nanoscale would help to establish a more robust assessment. If confirmed, such visual observations would represent a great step forwards for the soil science community. They would illustrate that microbial processing of litter-^{15}N favors its retention in soil thanks to interactions with mineral surfaces, and prevents it from being continuously cycled and eventually diluted, released and lost as inorganic ^{15}N.

Technical challenges to combine STXM and NanoSIMS

Several technical constraints, sometimes hard to reconcile, arise if the exact same spot on a given specimen has to be examined with STXM and NanoSIMS.

1) The samples must be mounted in the same fashion for STXM and NanoSIMS analysis. Most STXM holders contain either N (Si_3N_4 window) or C (TEM Cu grid with C lacey) and may introduce unwanted bias for NanoSIMS N and C imaging (ion scattering, background contribution).

2) The regions of interest (ROI) have to be large enough (about 500 nm in diameter) to achieve decent counting statistics with NanoSIMS; this is easier to do for large particles. At the same time, particles have to be transparent to X-rays, i.e. with an effective thickness smaller than 150 nm, to be studied by STXM. Consequently, flat particles are the best targets for joints STXM/NanoSIMS studies – with resulting issues in terms of biased sample populations.

3) Charging of quartz grains during NanoSIMS imaging, in spite of gold coating, is an issue, resulting in a dramatic decrease of signal intensity. This is usually addressed by flooding the sample with electrons for charge compensation using a device called “electron gun”. Because the electrons produced by the electron gun dazzle the detector for secondary electrons, the electron gun would have prevented us from acquiring the secondary electron images that were needed to overlap images obtained from STXM and NanoSIMS and to assess analytical bias. We decided to favor the secondary electron images and to mask, on our images, the very few regions showing obvious charging. As a consequence, there is no information at the location of charging while the information for the rest of the image is deemed suitable for interpretation. When mineral grains are significantly coated by organic material, charging effects can be neglected (see figure 1). As a result, only regions free of organic material appear to undergo charging; there is no significant loss of information about the OM at the surface of a microaggregate if charging obscures only the inorganic component.

Environmental Implications

Our study has demonstrated the feasibility of NanoSIMS investigations on isolated soil microstructures deposited on a clean surface. We have shown how NanoSIMS identifies organic and mineral components in microaggregates, detects the occurrence of local concentration of any isotopic label even in the case of weakly labeled samples. The observation of some label-rich hot spots in our long-term experiment shows that labeled organic matter in soil can be preserved over a long period.

STXM-NEXAFS combined with NanoSIMS generates more robust conclusions than NanoSIMS imaging alone. Joint STXM/NEXAFS analysis requires a significant amount of analytical time on both instruments. When implemented, the combination of methods offers a means to test hypothesis arising from bulk scale studies by visualizing the suspected process. The really unique set of results from such a combination, in addition to small-scale textural observation using SEM and TEM, opens a new window of opportunities for geochemical and ecological processes research at the sub-micron scale.

Acknowledgements

This research was financially supported by the France-Berkeley Fund. Johannes Lehmann, Jennifer Pett-Ridge and Jean-Nicolas Audinot are thanked for helpful discussion. We are also grateful to Sylvain Bernard for helpful advice and comments and David Kilcoyne for his support on the STXM beamline 5.3.2.2.Access to ALS beamline 5.3.2.2 was provided by the Office of Science, Office of Basic Energy Science (DE-AC02-05CH11231). We also thank three anonymous reviewers for their comments that improved the manuscript.

Supporting Information (SI) Available

Detailed information about the analytical parameters used for both STXM and NanoSIMS, sample preparation techniques, background information on the field study experiment, isotope reference standard analysis and additional images can be found in supplementary online information. This information is available free of charge via the Internet at http://pubs.acs.org/

References:

1. Ekschmitt, K.; Kandeler, E.; Poll, C.; Brune, A.; Buscot, F.; Friedrich, M.; Gleixner, G.; Hartmann, A.; Kastner, M.; Marhan, S.; Miltner, A.; Scheu, S.; Wolters, V., Soil-carbon preservation through habitat constraints and biological limitations on decomposer activity. *J. Plant Nutr. Soil Sci.* **2008**, *171*, 27-35.

2. Bos, R.; van der Mei, H. C.; Busscher, H. J., Physico-chemistry of initial microbial adhesive interactions - its mechanisms and methods for study. *FEMS Microbiol. Rev.* **1999**, *23*, (2), 179-229.

3. Lehmann, J.; Kinyangi, J.; Solomon, D., Organic matter stabilization in soil microaggregates: implications from spatial heterogeneity of organic carbon contents and carbon forms. *Biogeochemistry* **2007**, *85*, 45-57.

4. Mikutta, R.; Kaiser, K.; Dörr, N.; Vollmer, A. C.; Chadwick, O. A.; Chorover, J.; Kramer, C.; Guggenberg, G., Mineralogical impact on organic nitrogen across a long-term soil chronosequence (0.3–4100 kyr). *Geochim. Cosmochim. Acta* **2010**, *74*, 2142–2164.

5. Derrien, D.; Marol, C.; Balabane, M.; Balesdent, J., The turnover of carbohydrates in a cultivated soil estimated by 13C natural abundances. *Eur. J. Soil Sci.* **2006**, *57*, (4), 547-557.

6. von Lützow, M.; Kögel-Knabner, I.; Ekschmitt, K.; Flessa, H.; Guggenberg, G.; Matzner, E.; Marschner, B., SOM fractionation methods: Relevance to functional pools and stabilization mechanisms. *Soil Biol. Biochem.* **2007**, *39*, 2183-2207.

7. Grandy, A. S.; Neff, J. C., Molecular C dynamics downstream: The biochemical decomposition sequence and its impact on soil organic matter structure and function. *Sci. Total Environ.* **2008**, *404*, (2-3), 297-307.

8. Lechene, C. P.; Luyten, Y.; McMahon, G.; Distel, D. L., Quantitative Imaging of Nitrogen Fixation by Individual Bacteria Within Animal Cells. *Science* **2007**, *317*, (5844), 1563-1566.

9. Herrmann, A. M.; Clode, P. L.; Fletcher, I. R.; Nunan, N.; Stockdale, E. A.; O'Donnel, A. G.; Murphy, D. V., A novel method for the study of the biophysical interface in soils using nano-scale secondary ion mass spectrometry. *Rapid Commun. Mass Spectrom.* **2007**, *21*, (1), 29-34.

10. Heister, K.; Höschen, C.; Pronk, G.; Mueller, C.; Kögel-Knabner, I., NanoSIMS as a tool for characterizing soil model compounds and organomineral associations in artificial soils. *Journal of Soils and Sediments* **2012**, *12*, (1), 35-47.

11. Clode, P. L.; Kilburn, M. R.; Jones, D. L.; Stockdale, E. A.; Cliff, J. B.; Herrmann, A. M.; Murphy, D. V., In situ mapping of nutrient uptake in the rhizosphere using nanoscale sceondary ion mass spectrometry. *Plant Physiol.* **2009**, *151*, 1751-1757.

12. Popa, R.; Weber, P. K.; Pett-Ridge, J.; Finzi, J. A.; Fallon, S. J.; Hutcheon, I. D.; Nealson, K. H.; Capone, D. G., Carbon and nitrogen fixation and metabolite exchange in and between individual cells of Anabaena oscillarioides. *ISME* **2007**, *1*, (354-360).

13. Herrmann, A. M.; Ritz, K.; Nunan, N.; Clode, P. L.; Pett-Ridge, J.; Kilburn, M. R.; Murphy, D. V.; O'Donnell, A. G.; Stockdale, E. A., Nano-scale secondary ion mass spectrometry -- A new analytical tool in biogeochemistry and soil ecology: A review article. *Soil Biol. Biochem.* **2007**, *39*, (8), 1835-1850.

14. Mueller, C. W.; Kölbl, A.; Hoeschen, C.; Hillion, F.; Heister, K.; Herrmann, A. M.; Kögel-Knabner, I., Submicron scale imaging of soil organic matter dynamics using NanoSIMS - From single particles to intact aggregates. *Org. Geochem.* **2012**, *42*, (12), 1476-1488.

15. Brandes, J. A.; Lee, C.; Wakeham, S.; Peterson, M.; Jacobsen, C.; Wirick, S.; Cody, G., Examining marine particulate organic matter at sub-micron scales using scanning transmission X-ray microscopy and carbon X-ray absorption near edge structure spectroscopy. . *Mar. Chem.* **2004**, *92*, 107-121.

16. Solomon, D.; Lehmann, J.; Kinyangi, J.; Liang, B.; Heymann, K.; Dathe, L.; Hanley, K., Carbon (1s) NEXAFS spectroscopy of biogeochemically relevant reference organic compounds. . *Soil Sci. Soc. Am. J.* **2009**, *73*, (6), 1817-1830.

17. Kinyangi, J.; Solomon, D.; Liang, B.; Lerotic, M.; Wirick, S.; Lehmann, J., Nanoscale biogeocomplexity of organnomineral assemblage in soil: Application of STXM microscopy and C 1s-NEXAFS spectroscopy. *Soil Sci. Soc. Am. J.* **2006**, *70*, 1708-1718.

18. Bernard, S.; Benzerara, K.; Beyssac, O.; Brown, G. E.; Stamm, L. G.; Duringer, P., Ultrastructural and chemical study of modern and fossil sporoderms by Scanning Transmission X-ray Microscopy (STXM). *Rev. Palaeobot. Palynology* **2009**, *156*, (1-2), 248-261.

19. De Gregorio, B. T.; Stroud, R. M.; Nittler, L. R.; Alexander, C. M. O. D.; Kilcoyne, A. L. D.; Zega, T. J., Isotopic anomalies in organic nanoglobules from Comet 81P/Wild 2: Comparison to Murchison nanoglobules and isotopic anomalies induced in terrestrial organics by electron irradiation. *Geochim. Cosmochim. Acta* **2010**, *74*, (15), 4454-4470.

20. Zeller, B.; Colin-Belgrand, M.; Dambrine, E.; Martin, F., Fate of nitrogen released from 15N-labeled litter in European beech forests. *Tree Physiology* **2001**, *21*, (2-3), 153-162.

21. Hatton, P.-J.; Kleber, M.; Zeller, B.; Moni, C.; Plante, A.; Townsend, K.; Lajtha, K.; Derrien, D., Transfer of a ^{15}N litter label from the organic surface layer (O) to mineral-organic associations in the A-horizon: a decadal perspective. *Org. Geochem.* **2012**, *42*, (12), 1489-1501.

22. Hitchcock, A. P. *aXis2000. Analysis of X-ray Images and Spectra*, McMaster University, Hamilton, Ontario, Canada.: **2006**.

23. McMahon, G.; Saint-Cyr, H. F.; Lechene, C.; Unkefer, C. J., CN- Secondary Ions Form by Recombination as Demonstrated Using Multi-Isotope Mass Spectrometry of 13C- and 15N-Labeled Polyglycine. *J. Am. Soc. Mass Spectrom.* **2006**, *17*, (8), 1181-1187.

24. Gnaser, H., Formation of metastable N2- and CO- anions in sputtering. *Phys. Rev. A* **1997**, *56*, (4), R2518.

25. Thomen, A.; Remusat, L.; Robert, F.; Meibom, A.; Mostefaoui, S., Chemical and Nitrogen Isotopic Composition of the Hotspots in Orgueil Insoluble Organic Matter. In *Lunar and Planetary Institute Science Conference*, **2010**; 2472.pdf.

26. Luo, X. J.; Guillot, J.; Sanctuary, R.; Migeon, H. N., Topography artefacts in NanoSIMS 50 elemental images. In *7th European Workshop on Secondary Ion Mass Spectrometry*, Munster, **2010**; #20.

27. Lee, J. L. S.; Gilmore, I. S.; Fletcher, I. W.; Seah, M. P., Topography and field effects in the quantitative analysis of conductive surfaces using ToF-SIMS. *Appl. Surf. Sci.* **2008**, *255*, (4), 1560-1563.

28. Keiluweit, M.; Nico, P.; Johnson, M. G.; Kleber, M., Dynamic molecular chemical strucutre of plant biomass-derived black carbon (biochar). *Environ. Sci. Technol.* **2010**, *44*, 1247-1253.

29. Lawrence, J. R.; Swerhone, G. D. W.; Leppard, G. G.; Araki, T.; Zhang, X.; West, M. M.; Hitchcock, A. P., Scanning Transmission X-Ray, Laser Scanning, and Transmission Electron Microscopy Mapping of the Exopolymeric Matrix of Microbial Biofilms. *Appl. Environ. Microbiol.* **2003**, *69*, (9), 5543-5554.

30. Lehmann, J.; Solomon, D.; Kinyangi, J.; Dathe, L.; Wirick, S.; Jacobsen, C., Spatial complexity of soil organic matter forms at nanometre scales. *Nature geoscience* **2008**, *1*, 238-242.

31. Chan, C. S.; Fakra, S. C.; Edwards, D. C.; Emerson, D.; Banfield, J. F., Iron oxyhydroxide mineralization on microbial extracellular polysaccharides. *Geochim. Cosmochim. Acta* **2009**, *73*, 3807-3818.

Figure 1: NanoSIMS images of a soil micro aggregate, indicating the location of ^{12}C, ^{26}CN and ^{18}O along the particle, which shape is shown by secondary electrons. Maps of $\delta^{13}C$ and $\delta^{15}N$ are also represented. ^{15}N-rich hot spots can be distinguished with $\delta^{15}N$ significantly above the natural abundance; $\delta^{15}N$= 573±175 ‰, 382±85 ‰ and 467±130 ‰ (2 sigma errors) for a, b and c, respectively. A mask was applied to these images by taking in account only the area of the particle with $^{12}C^-$ and $^{26}CN^-$ counts above an arbitrary threshold. Then, black regions correspond to the location of the Si_3N_4 window (on the sides) or to area where we cannot get reliable data. $\delta(\text{in ‰}) = (R_{sample}/R_{standard} - 1) \times 1000$.

Figure 2: Example of the combined study of a soil aggregate by NanoSIMS (A and B) and STXM/NEXAFS (C and D). ^{18}O image (A) can be used to map the inorganic part of the whole particle. OM, represented by ^{12}C and ^{26}CN, occurs only as a rim around the particle (B). Color scale for A and B is similar to figure 1. (C) is an image of C and N as revealed by STXM imaging, the regions were the sample was to thick to get NEXAFS spectra or was free of organic matter appear in grey. In (D), the

NEXAFS spectra of 3 areas are compared with a black carbon spectra obtained from [28]. Area (1) is identified by C-NEXAFS as black carbon; this is consistent with a strong $^{12}C^-$ signal on the NanoSIMS image. See text for peaks identification.

Figure 3: Joined NanoSIMS/STXM study of a soil aggregate with a ^{15}N hot spot. (A): ^{26}CN image. (B): $\delta^{15}N$ image of the same grain. A mask was applied on these images with a similar fashion as figure 2. The point (1) indicates a ^{15}N-rich hot spot, $\delta^{15}N=213\pm132‰$. STXM C and N imaging is reported in (C). NEXAFS (panel D) shows that the litter-derived-^{15}N (region 1) would be involved in microbial OM as indicated by the comparison with forest litter from [30] and microbe cell from [31]. See text for peak identification.

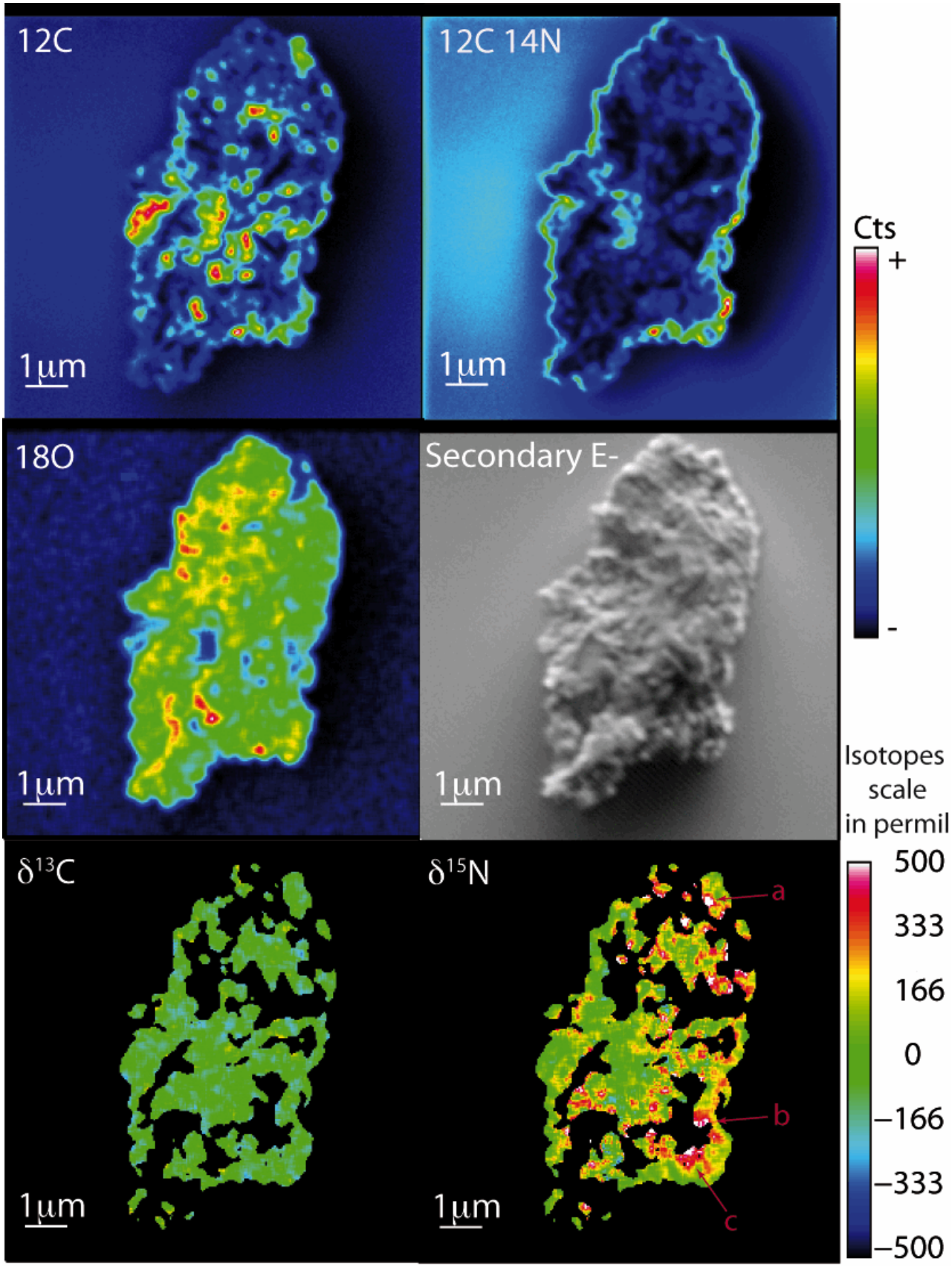
12C
1µm
12C 14N
1µm
Cts
+
-
18O
1µm
Secondary E-
1µm
Isotopes
scale
in permil
δ13C
1µm
δ15N
1µm
a
b
c
500
333
166
0
−166
−333
−500

Figure 1

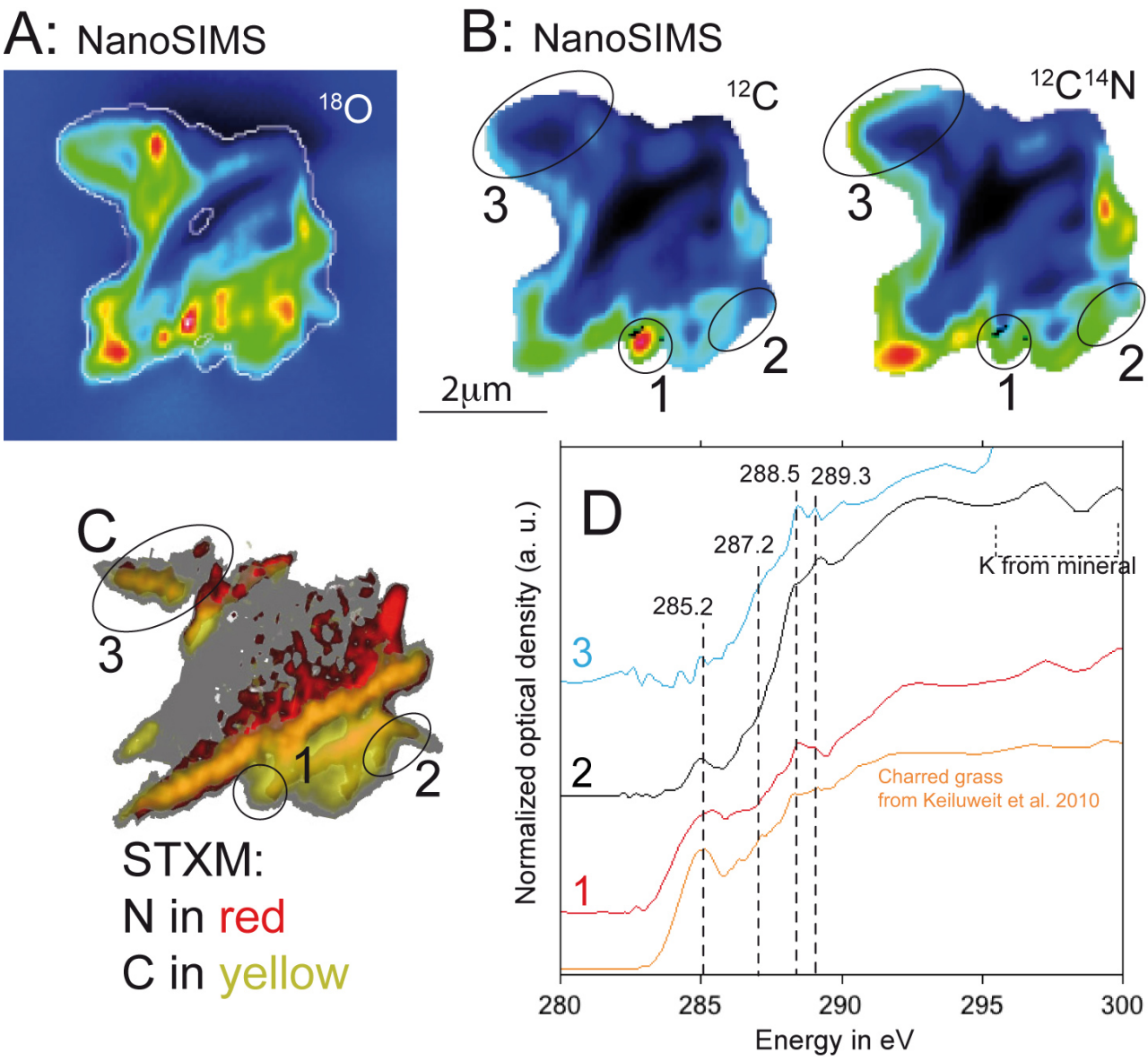
A: NanoSIMS
18O
B: NanoSIMS
12C
12C14N
3
2
1
2μm
C
STXM:
N in red
C in yellow
D
288.5
289.3
287.2
285.2
K from mineral
Charred grass
from Keiluweit et al. 2010
Normalized optical density (a. u.)
Energy in eV
280
285
290
295
300

Figure 2

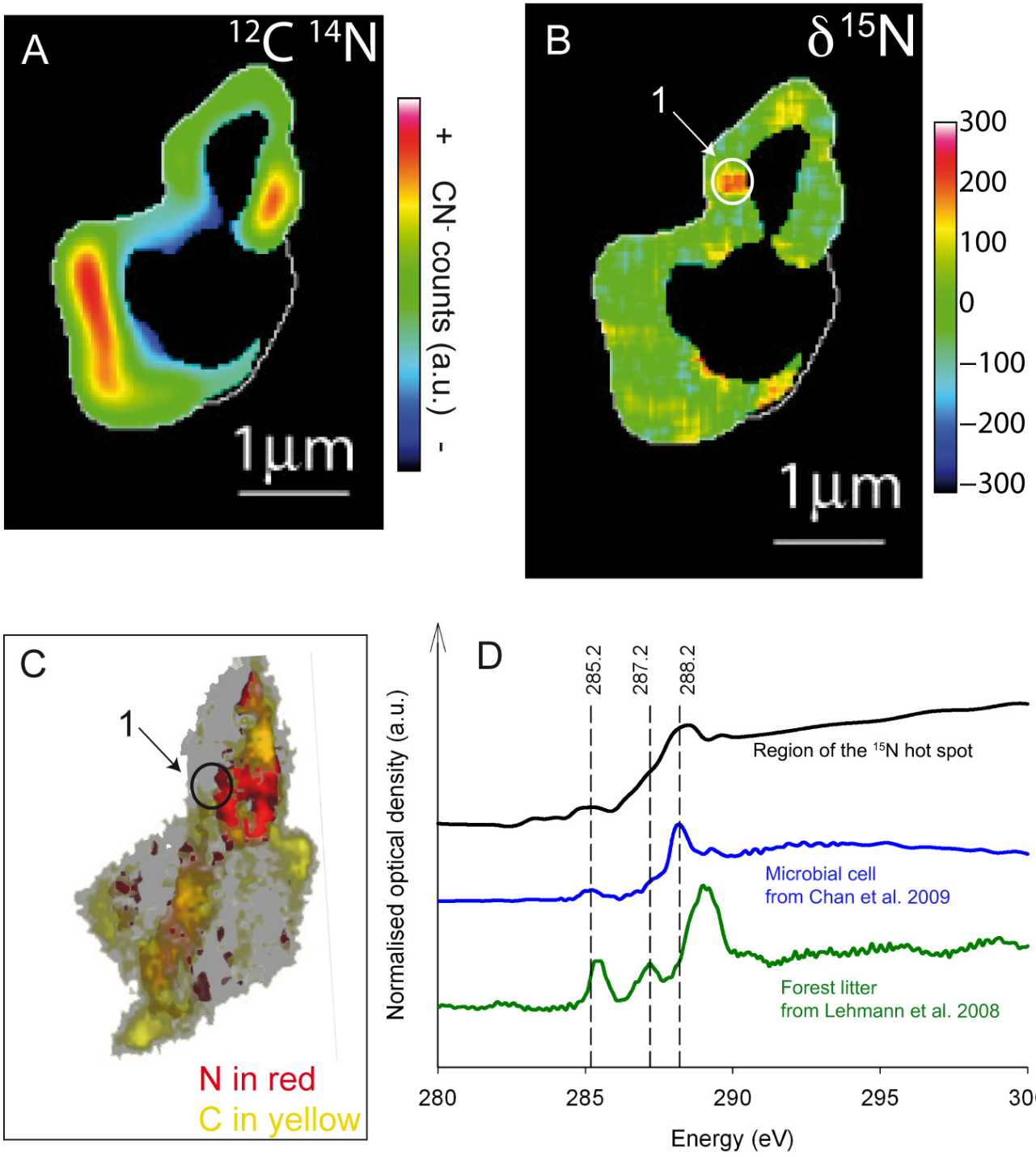
A
^{12}C ^{14}N
1µm
+
CN- counts (a.u.)
-
B
δ ^{15}N
1
1µm
300
200
100
0
−100
−200
−300
C
1
N in red
C in yellow
D
285.2
287.2
288.2
Region of the ^{15}N hot spot
Microbial cell
from Chan et al. 2009
Forest litter
from Lehmann et al. 2008
Normalised optical density (a.u.)
280
285
290
295
300
Energy (eV)

Figure 3